New Alternating Ferro- and Antiferromagnetic One-Dimensional Complexes. Synthesis, Characterization, Crystal Structure, and Magnetic Properties of [M(4,4′-dimethylbipyridine)(N₃)₂]ₙ [M = Cu(II), Mn(II), Ni(II), Fe(II)]

Hao-Yu Shen,[†,‡] Wei-Ming Bu,[§] En-Qing Gao,[‡] Dai-Zheng Liao,*,[‡] Zong-Hui Jiang,[∥] Shi-Ping Yan,[‡] and Geng-Lin Wang[‡]

Department of Chemistry, Nankai University, Tianjin, 300071, P. R. China, Laboratory of Supramolecular Chemistry and Spectroscopy, Jilin University, Changchun, Jilin Province, 130023, P. R. China, and State Key Laboratory of Coordination Chemistry, Nanjing University, Nanjing, 210008, P. R. China

The preparation, X-ray crystal structure, and magnetic properties of alternating 1,1- and 1,3-azido-bridged copper-(II) complex [Cu(4,4′-dmbpy)(N₃)₂]ₙ (**1**, 4,4′-dmbpy = 4,4′-dimethylbipyridine) have been reported. It crystallizes in triclinic system, space group $P\bar{1}$, $a = 7.9903(1)$ Å, $b = 9.3545(9)$ Å, $c = 10.754(2)$ Å, $\alpha = 113.485(1)°$, $\beta = 101.399(1)°$, $\gamma = 101.897(1)°$, $Z = 2$. The magnetic properties of **1** have been investigated in the temperature range 1.5−300 K. Alternating antiferromagnetic ($-J = 191.0$ cm⁻¹) interaction through a 1,3-N₃⁻ bridge and ferromagnetic ($J = 297.1$ cm⁻¹) interaction through a 1,1-N₃⁻ bridge are obtained for **1** by analyzing the magnetic susceptibility data with the Hamiltonian $\hat{H} = -J\sum(\hat{S}_{2i}\hat{S}_{2i-1} - \alpha\hat{S}_{2i}\hat{S}_{2i+1})$. It's derivatives ({Mn(4,4′-dmbpy)(N₃)₂}ₙ (**2**), {Ni(4,4′-dmbpy)(N₃)₂}ₙ (**3**), and {Fe(4,4′-dmbpy)(N₃)₂}ₙ (**4**) and the heterometallic derivatives {NiMn(4,4′-dmbpy)₂(N₃)₄}ₙ (**5**) and {CuMn(4,4′-dmbpy)₂(N₃)₄}ₙ (**6**) have also been synthesized and characterized by electronic and IR spectra. The X-ray powder diffraction and the magnetic properties of **6** have also been discussed.

Introduction

Coordination metal complexes with one-dimensional structures have long been investigated as materials with unusual properties. Molecular-based ferromagnets, conductors, and nonlinear optical materials represent several applications of one-dimensional coordination polymers. It is possible to modify the bulk magnetic, electronic, and optical properties of such materials by tailoring the consistent molecules.[1−10] Compared with high-dimensional compounds, one-dimensional molecule-based magnetic materials have larger anisotropy, which is attributed to stronger coercive field and broader hysteresis loop, favoring hard magnetic materials. The distinctive properties of some one-dimensional materials, such as metamagnetism, spin glass, and spin liquid, are important in the fields of quantum mechanics and experimental and theoretical solid-state science. The studies on this area have been carried out all over the world.[11−13]

The studies of azido-bridged complexes have been a focus of molecular-based magnetic studies for many years because azide ions have two possible bridging modes: end-to-end (EE) and end-on (EO). EE is known to favor antiferromagnetic interaction, while EO favors ferromagnetic interactions. The ferromagnetic behavior of the compounds with EO bridges has been explained by Kahn with the spin-polarization concept for small angles (<108° for copper(II))[14,15] and the mechanism of the coexist of spin-delocalization and spin-polarization based on neutron diffraction studies and density functional theoretical calculation.[16]

Although the 1,1-azido bridges favor antiferromagnetical interactions when ∠Cu−N−Cu is larger than 108°, some complexes with net ferromagnetical interaction have been obtained, such as one-dimensional complexes with ∠Cu−N−Cu = 119.5°, $J = 26$ cm⁻¹ and ∠Cu−N−Cu = 111.9°, $J = 75$ cm⁻¹.[17,18] For 1,3-azido bridges, the magnetostructural correlation indicates the magnitude of the antiferromagnetic coupling is generally related to the angle of Cu−N−N and the torsion angle of Cu−N₃−Cu.[19]

(1) Chen, C. T.; Suslick, K. S. *Coord. Chem. Rev.* **1993,** *128,* 293.
(2) Kahn, O. *Molecular magnetism;* VCH Publishers: New York, 1993.
(3) Miller, J. S. Ed. *Extended Linear Chain Compounds*; Plenum: New York, 1982, Vol. 3.
(4) Delhaes, P.; Drillon, M. Eds. *Organic and Inorganic Linear Dimensional Crystalline Materials.* NATO ASI Ser. 168; NATO: New York, 1989.
(5) Nakatani, K.; Bergeral, P.; Codjovi, E. *Inorg. Chem.* **1991,** *30,* 3977.
(6) Schneider, O.; Hanack, O. *Angew. Chem., Int. Ed. Engl.* **1982,** *19,* 79.
(7) Hanck, M.; Deger, S.; Lange, A. *Coord. Chem. Rev.* **1988,** *83,* 115.
(8) Hank, M.; Gul A.; Subramanian, L. R. *Inorg. Chem.* **1992,** *31,* 1542.
(9) Alferness, R. C. *Science* **1986,** *234,* 825.
(10) Eaton, D. *Science* **1991,** *253,* 281.

(11) Haldane, F. D. M. *Phys. Rev. Lett.* **1983,** *50,* 1153.
(12) Shiba, H.; Sakai, T.; Luthi, B. *J. Magn. Magn. Mater.* **1995,** *104−144,* 1590.
(13) Bramwell, S. T. *Annu. Rep. progr.Chem. Sect. A.* **1997,** *93,* 457.
(14) Thompson, L. K.; Tandon, S. S. *Comments Inorg. Chem.* **1996,** *18,* 125.
(15) Charlot, M.-F.; Kahn, O.; Chaillet, M.; Larrieu, C. *J. Am. Chem. Soc.* **1986,** *108,* 2574.
(16) Aebersold, M. A.; Gillon, B.; Plantevin, O.; Kahn, O. *J. Am. Chem. Soc.* **1998,** *120,* 5238.
(17) Thompson, L. K.; Tandon, S. S.; Lloret, F.; Cano, J.; Julve, M. *Inorg. Chem.* **1997,** *36,* 3301.
(18) Escuer, A.; Vicente, R.; Mautner, F. A.; Goher, M. A. S. *Inorg. Chem.* **1997,** *36,* 1233.

In contrast with the abundant number of binuclear copper(II)[20−25] or one-dimensional nickel(II)[26−29] complexes with azide bridging ligands, the studies on the magnetochemistry of alternating 1,1- and 1,3-azido-bridged one-dimensional copper(II) compounds are still rare. Herein we report the synthesis and characterization of a series of new alternating linear compounds [M(4,4′-dmbpy)(N₃)₂]ₙ (4,4′-dmbpy = 4,4′-dimethylbipyridine; M = Cu(II), **1**; Mn(II), **2**; Ni(II), **3**; Fe(II), **4**) and the heterometallic compounds {NiMn(4,4′-dmbpy)₂-(N₃)₄}ₙ (**5**) and {CuMn(4,4′-dmbpy)₂(N₃)₄}ₙ (**6**) and the crystal structure of **1**. The magnetic studies on **1** and **6** are also reported.

Experimental Section

Synthesis. [Cu(4,4′-dmbpy)(N₃)₂]ₙ (**1**) was prepared by the following method. A solution of 4,4′-dimethylbipyridine (26.9 mg, 0.2 mmol) in methanol (10 mL) was added dropwise to a stirred aqueous solution (10 mL) of Cu(OAc)₂ (40 mg, 0.2 mmol); then NaN₃ (26 mg 0.4 mmol) dissolved in water (10 mL) was added slowly. All the insoluble products were filtrated and the clear green solution was left to stand undisturbed at room temperature. Several months later, X-ray qualified dark green single crystals were obtained, which were filtered, washed with water, methanol, and ether, and dried in a vacuum to yield 65%.

The powder products [Mn(4,4′-dmbpy)(N₃)₂]ₙ (**2**), [Ni(4,4′-dmbpy)-(N₃)₂]ₙ (**3**), [Fe(4,4′-dmbpy)(N₃)₂]ₙ (**4**), {NiMn(4,4′-dmbpy)₂(N₃)₄}ₙ (**5**), and {CuMn(4,4′-dmbpy)₂(N₃)₄}ₙ (**6**) were prepared by a similar method, using Mn(OAc)₂, Ni(OAc)₂, FeSO₄·7H₂O or a mixture solution of Mn(OAc)₂ and Ni(OAc)₂ or Cu(OAc)₂ instead of Cu(OAc)₂. In the case of the Fe(II) complex, vitamin C (∼10 mg) was added to protect Fe(II) from oxidation.

Spectral and Magnetic Measurements. Elemental analyses of carbon, hydrogen, and nitrogen were carried out with a Perkin-Elmer analyzer model 240. The electronic spectrum was measured with a Shimadzu UV-2101PC UV−vis scanning spectrophotometer. The infrared spectroscopy on KBr pellets was performed on a Nicolet 5DX FT-IR spectrophotometer in the 4000−400 cm⁻¹ region. Molar conductances were measured in 10⁻³ mol dm⁻³ DMF solutions, using a DDS-11A conductometer. Magnetic susceptibility measurements of crystalline sample for **1** and powder sample for **6** were carried out in the temperature range 1.5−300 K on a vibrating sample magnetometer, model CF-1.

X-ray Crystallography. The X-ray single-crystal data were collected on a computer-controlled Siemens P4 diffractometer equipped with a graphite-monochromatized Mo−Kα radiation (λ = 0.71073 Å) and a crystal of size 0.13 × 0.27 × 0.38 mm. The crystallographic data, conditions for the collection of intensity data, and some features of the structure refinements are listed in Table 1. Cell parameters were determined by least-squares calculations based on the setting angles and 33 reflections with θ angles ranging from 4.45 to 12.37° at 293(2) K. A total of 2304 independent reflections were measured (*I* > 2σ(*I*)). No absorption correction was made during processing. Hydrogen atoms were added theoretically and refined with riding model position

(19) Sikorov, S.; Bkouche-Waksman, I.; Kahn, O. *Inorg. Chem.* **1984**, *23*, 490.
(20) Thompson, L. K.; Tandon, S. S.; Manuel, M. E. *Inorg. Chem.* **1995**, *34*, 2356.
(21) Kahn, O.; Sikorav, S.; Gouteron, J.; Jeannin, S.; Jeannin, Y. *Inorg. Chem.* **1983**, *22*, 2877.
(22) Comarmond, P.; Plumere, P.; Lehn, J.-M.; Agnus, Y.; Louis, R.; Weiss, R.; Kahn, O.; Morgenstern-Badarau, I. *J. Am. Chem. Soc.* **1982**, *104*, 6330.
(23) Tandon, S.; Thompson, L. K.; Manuel, M. E.; Bridson, J. N. *Inorg. Chem.* **1994**, *33*, 5555.
(24) Chaudhuri, P.; Oder, K.; Wieghardt, K.; Nuber, B.; Weiss, J. *Inorg. Chem.* **1986**, *25*, 2818.
(25) Felthouse, T. R.; Hendrickson, D. N. *Inorg. Chem.* **1978**, *17*, 444.
(26) Vicente, R.; Escuer, A. *Polyhedron* **1995**, *14*, 2133.
(27) Cortes, R.; Urtiaga, K.; Lezama, L.; Pizarro, J. L.; Goni, A.; Arriortua, M. I.; Rojo, T. *Inorg. Chem.* **1994**, *33*, 4009.
(28) Escuer, A.; Vicente, R.; Ribas, J.; Fallah, M. S. E.; Solans, X.; Font-Bardia, M. *Inorg. Chem.* **1994**, *33*, 1842.
(29) Escuer, A.; Vicente, R.; Ribas, J.; Fallah, M. S. E.; Solans, X.; Font-Bardia, M. *Inorg. Chem.* **1993**, *32*, 3727.

Table 1. Crystal Data for [Cu(4,4′-dmbpy)(N₃)₂]ₙ **1**[a]

empirical formula	C₁₂H₁₂CuN₈
fw	331.84
T	293(2)K
λ	0.71073 Å
space group	P1̄
unit cell dimens	*a* = 7.9903(1) Å, α = 113.485(1)°
	b = 9.3545(9) Å, β = 101.399(1)°
	c = 10.754(2) Å, γ = 101.897(1)°
vol	685.4(2) Å³,
Z	2
ρ_obsd	1.625 g/cm³
ρ_cacld	1.608 g/cm³
abs coeff	1.600 mm⁻¹
final *R* indices [*I* > 2σ(*I*)]	R1 = 0.0434, wR2 = 0.1129
R indices (all data)	R1 = 0.0568, wR2 = 0.1297

[a] R1 = ∑||F_o| − |F_c||/∑|F_o|; wR2 = [∑(w(F_o² − F_c²)²)/∑(w(F_o²)²)]^{1/2}; w = 1/[σ²(F_o²) + (0.0633P)² + 0.0000P], where P = (F_o² + 2F_c²)/3.

Table 2. Selected Bond Length (Å) and Angles (deg) for [Cu(4,4′-dmbpy)(N₃)₂]ₙ[a]

Cu−N(4)	1.971(5)	Cu−N(8)	2.027(4)
Cu−N(1)	1.987(5)	Cu−N(6)B	2.521(6)
Cu−N(7)	2.021(4)	Cu−N(1)A	2.621(6)
Cu−CuA	3.481(2)	Cu−CuB	5.420(1)

N(4)−Cu−N(1)	95.5(2)	N(6)B−Cu−N(1)A	173.4(2)
N(4)−Cu−N(7)	171.2(2)	N(4)−Cu−CuA	93.8(2)
N(1)−Cu−N(7)	92.9(2)	N(1)−Cu−CuA	48.3(2)
N(4)−Cu−N(8)	92.0(2)	N(7)−Cu−CuA	89.83(12)
N(1)−Cu−N(8)	172.1(2)	N(8)−Cu−CuA	128.65(14)
N(7)−Cu−N(8)	79.5(2)	N(6)B−Cu−CuA	139.6(2)
N(4)−Cu−N(6)B	92.7(2)	N(1)A−Cu−CuA	34.48(10)
N(1)−Cu−N(6)B	91.4(2)	N(2)−N(1)−Cu	121.3(4)
N(7)−Cu−N(6)B	89.7(2)	N(3)−N(2)−N(1)	177.5(7)
N(8)−Cu−N(6)B	90.9(2)	N(5)−N(4)−Cu	125.9(4)
N(4)−Cu−N(1)A	90.9(2)	N(6)−N(5)−N(4)	177.3(7)
N(1)−Cu−N(1)A	82.8(2)	N(8)−Cu−N(1)A	94.5(2)
N(7)−Cu−N(1)A	87.6(2)		

[a] Symmetry transformations used to generate equivalent atoms: B, −x + 2, −y, −z + 1; A, −x + 1, −y, −z + 1.

Table 3. Unit Cell Parameters in the P1̄ Space Group for **1** and **6**

	1		
cell parameters	single crystal	powder pattern	6
a (Å)	7.9903	8.0356	8.0189
b (Å)	9.3545	9.3731	9.3572
c (Å)	10.754	10.7843	10.7628
α (deg)	113.485	113.442	113.688
β (deg)	101.399	101.509	101.996
γ (deg)	101.897	101.923	101.607

parameters and fixed with isotropic thermal parameters. The structure was solved by direct method (SHELX86)[30,31] and refined by the full-matrix least-squares method with use of the SHELXL-93 package of program. The final refinement was by full-matrix least-squares on *F*². The final R1 = 0.0434, wR2 = 0.1129 (*I* > 2σ(*I*)), R1 = 0.0568, wR2 = 0.1297 (all data), and S = 1.034. The largest peak and hole on the final difference Fourier map had the value of 0.441 and −0.548 e Å⁻³, respectively. Significant bond parameters are given in Table 2.

The X-ray powder diffraction profiles were recorded at room temperature on a Rigakudmax diffractometer using Cu Kα radiation. The X-ray powder patterns of compound **1** and **6** were found to be very close to that of the crystal **1**. The reflections of **1** and **6** were indexed and the unit cell parameters were refined in P1̄ space group. The cell parameters are given in Table 3.

Results and Discussion

Composition and Physical Properties of 1−6. The elemental analysis results are listed in Table 4. The general physical

(30) SPD-PLUS, Enraf-Nonius, Delft, The Netherlands, 1985.
(31) Sheldrick, G. M. *Acta Crystallogr.* **1990**, *A46*, 467.

Table 4. Elemental Analysis Results for **1**−**6**

no.	complex	C	H	N	M
1	$C_{12}H_{12}N_8Cu$	43.31 (43.44)	3.64 (3.65)	33.74 (33.77)	19.30 (19.15)
2	$C_{12}H_{12}N_8Mn$	44.78 (44.59)	3.28 (3.74)	34.55 (34.67)	17.28 (17.00)
3	$C_{12}H_{12}N_8Ni$	44.12 (44.08)	3.85 (3.70)	34.34 (34.27)	17.68 (17.95)
4	$C_{12}H_{12}N_8Fe$	44.26 (44.47)	3.52 (3.74)	34.52 (34.57)	17.02 (17.23)
5	$C_{24}H_{24}N_{16}MnNi$	44.12 (44.34)	3.68 (3.72)	34.22 (34.47)	8.22^a 9.42^b (8.45) (9.03)
6	$C_{24}H_{24}N_{16}CuMn$	44.26 (44.01)	3.42 (3.69)	34.05 (34.25)	8.24^a 9.44^c (8.39) (9.70)

^{a} Mn(II). ^{b} Ni(II). ^{c} Cu(II).
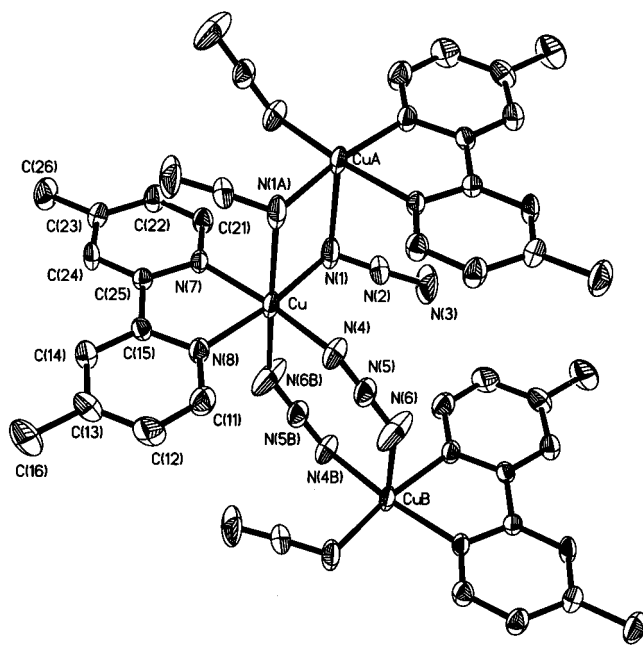
Figure 1. The ORTEP drawing of [Cu(4,4′-dmbpy)(N$_3$)$_2$]$_n$.

properties are listed in Table 5, and the molar conductance values for the complexes in DMF indicate that all the complexes are nonelectrolytes.[32]

Crystal Structure of [Cu(4,4′-dmbpy)(N₃)₂]ₙ (1). An ORTEP drawing of the one-dimensional complex [Cu(4, 4′-dmbpy)-(N$_3$)$_2$]$_n$ and the view of the unit cell are shown in Figures 1 and 2, respectively. The crystal structure consists of chains of Cu(II) ions alternatively linked by two EE [Cu−N(4) = 1.971(5) Å, Cu−N(6)B = 2.521(6) Å], and two EO [Cu−N(1) = 1.987(5) Å, Cu−N(1)A = 2.621(6) Å] azido bridges, which is similar to that of the compound Cu(3-pic)$_2$(N$_3$)$_2$ (3-pic = 3-picoline).[33] All Cu−N distances fall in the ranges 1.94−2.06 and 2.050−2.080 Å for short and long distances, respectively, which are very close to corresponding distance reported for copper(II) azido complex.[33−39] Each copper(II) ion has a
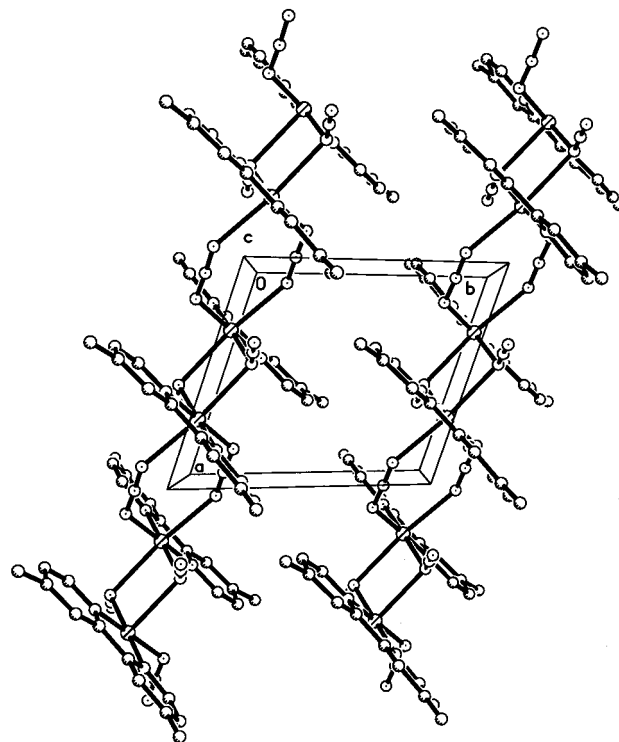
Figure 2. The view of the crystal cell of [Cu(4,4′-dmbpy)(N$_3$)$_2$]$_n$.

distorted octahedral coordination, completed by the two nitrogen atoms of the 4,4′-dimethylbipyridine ligand [Cu−N(7) = 2.021(4) Å, Cu−N(8) = 2.027(4) Å]. The EO and EE bridges are arranged cis, being almost perpendicular to each other [N(4)−Cu−N(1)A = 90.9(2)°, N(4)−Cu−N(1) = 95.2(2)°, N(1)−Cu−N(6)B = 91.4(2)°, N(1)−Cu−N(1)A = 82.8(2)°]. The nitrogen atom, N(1)A of the EO bridge, N(6)B of the EE bridge, and the copper atom are almost in a line [N(1)A−Cu−N(6)B = 173.4(2)°], which indicates Cu(II) is located in a elongated octahedral environment. N(1), N(4), N(8), and N(7) form the main plane of the octahedron (plane 1), and the Cu atom slightly deviates from it (0.0421 Å). The Cu−N(1)−CuA−N(1)A bridging unit forms another plane (plane 2). The EO bridging azides, which are quasilinear [N(3)−N(2)−N(1) = 177.5(7)°], deviate slightly (up or down) from plane 2. The dihedral angle between planes 1 and 2 is 88.4°. Cu, CuB, N(4)−N(6), and N(4)−N(6)B form plane 3. The dihedral angles between planes 1 and 3 and planes 2 and 3 are 89.9° and 93.9°, respectively. The results show that the three planes are almost perpendicular to one another. The Cu−N(1)−CuA angle for EO bridge is 97.2°. Ferromagnetic coupling of Cu(II) ions mediated by EO bridges can be expected. The N(5)−N(4)−Cu angle is 125.9(4)° and CuB−N(6)−N(5) is 137.0° for EE bridges, with the torsion angle of the Cu−(N$_3$)$_2$−Cu unit being 0°. The intrachain Cu···Cu distance is 3.481 and 5.420 Å in the EO and EE bridges, respectively.

The shortest distance between 4,4′-dmbpy ligands from two neighboring chains is separated by approximately 8 Å, which indicates no π−π interaction through 4,4′-dmbpy ligands in the neighboring chains.

IR and Electronic Spectra. The characteristic absorptions for IR and electronic spectra (solid) are listed in Table 6. There are strong absorptions at ∼2100 cm^{-1} in the IR spectra of **1**−**6**,

(32) Geary, W. T. *Coord. Chem. Rev.* **1971**, *12*, 13.
(33) Mautner, F. A.; Goher, M. A. S. *Polyhedron* **1992**, *11*, 2537.
(34) Vicente, R.; Escuer, A.; Ferretjans, J.; Stoeckli-Evans, H.; Solans, X.; Font-Bardia, M. *J. Chem. Soc., Dalton Trans.* **1997**, 167.
(35) Escuer, A.; Vicente, R.; Fallah, M. S. E.; Goher, M. A. S.; Mautner, F. A. *Inorg. Chem.* **1998**, *37*, 4466.
(36) Goher, M. A. S.; Mautner, F. A. *Polyhedron* **1998**, *17*, 1561.
(37) Rojo, T.; Larramendi, J. I. R.; Duran, I.; Mesa, J. L.; Via, J.; Arriortua, M. I. *Polyhedron* **1990**, *9*, 2693.

(38) Real, J. A.; Ruiz, R.; Faus, J.; Lloret, F.; Julve, M.; Journaux, Y.; Philoche-Levisalles, M.; Bois, C. *J. Chem., Soc., Dalton Trans.* **1994**, 3769.
(39) Tuczek, F.; Bensch, W. *Inorg. Chem.* **1995**, *34*, 1482.

Table 5. Physical Properties of **1**–**6**

no.	complex	yield %	mp/°C	color, state	molar conductance (s cm^{-1} mol^{-1})
1	Cu(4,4′-dmbpy)(N₃)₂	65	>280	dark green crystal	0.68
2	Mn(4,4′-dmbpy)(N₃)₂	63	>280	light yellow powder	0.69
3	Ni(4,4′-dmbpy)(N₃)₂	58	>280	light green powder	0.85
4	Fe(4,4′-dmbpy)(N₃)₂	45	>280	dark green powder	0.56
5	MnNi(4,4′-dmbpy)₂(N₃)₄	68	>280	light blue powder	0.58
6	CuMn(4,4′-dmbpy)₂(N₃)₄	54	>280	dark green powder	0.62

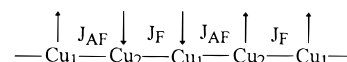**Table 6.** Characteristic Absorptions of IR and Electronic Spectra of **1**–**6**

no.	compound	IR (KBr)/cm^{-1}			UV−vis/nm	
		$\nu(N_3^-)$	ν(4,4′-dmbpy)	$\nu(N_3^-)$	$\pi-\pi$	d−d
1	Cu(4,4′-dmbpy)(N₃)₂	2115, 2110	1600, 1550, 1450, 1020, 940, 850	1290	272.8, 398.2	658.2
2	Mn(4,4′-dmbpy)(N₃)₂	2125, 2080	1620, 1560, 1450, 1030, 950, 860	1295	270.0, 392.2	−
3	Ni(4,4′-dmbpy)(N₃)₂	2120, 2105	1600, 1560, 1460, 1030, 940, 860	1300	284.0, 388.5	660.0
4	Fe(4,4′-dmbpy)(N₃)₂	2110, 2080	1610, 1550, 1450, 1025, 955, 855	1295	278.2, 400.2	580.0
5	MnNi(4,4′-dmbpy)₂(N₃)₄	2120, 2110	1600, 1565, 1460, 1025, 945, 860	1290	268.8, 396.2	662.8
6	CuMn(4,4′-dmbpy)₂(N₃)₄	2115, 2100	1620, 1555, 1460, 1030, 950, 845	1300	266.2, 398.8	658.2
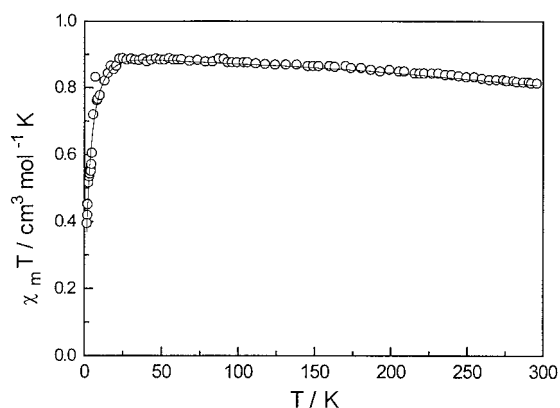
Figure 3. Plots of the products $\chi_m T$ vs temperature for [Cu(4,4′-dmbpy)(N₃)₂]ₙ. The solid line represents the best fitting (see text for the fitted parameters).

which can be attributed to the characteristic absorptions of $\nu_{as}(N_3^-)$, The bands in the region of 1360−1280 cm^{-1} are attributed to $\nu_s(N_3^-)$. These facts show that there are EO and EE azido bridges in **1**−**6**,[40,41] which is in agreement with the crystal structure of **1**. There are some characteristic bands for 4,4′-dmbpy in the region of ∼1600, 1550, 1450, 940, and 850 cm^{-1} for **1**−**6**.

There are two absorptions at λ = ∼270, ∼390 nm in the electronic spectra for all the six complexes, which can be assigned to the $\pi-\pi$ transition (∼270 nm) and the metal to ligand transition(∼390 nm). The bands in the visible region for **1**, **3**, and **4** can be assigned to d−d transitions of the metal ions. No absorption in the visible region is observed for compound **2**, which is due to the fact that all possible transitions for Mn(II) ions in the octahedral environment are all spin-forbidden. Those of **5** and **6** can be regarded as the overlap of the d−d transition of two kinds of metal ions. Because both **5** and **6** contain Mn(II) ions, the bands in the visible region for **5** and **6** can be assigned to the d−d transitions of Ni(II) and Cu(II) ions, respectively.

Magnetic Studies. The magnetic behavior of [Cu(4,4′-dmbpy)(N₃)₂]ₙ (**1**) has been studied and is represented in Figure 3, in the form of $\chi_m T$ vs T plots. The observed $\chi_m T$ value is 0.815 cm^3 K mol^{-1} at 295.8 K, which is slightly higher than the spin-only value of 0.75 cm^3 K mol^{-1} for two uncoupled

Scheme 1. The Relationship of the Magnetic Exchange Coupling of **1**.

$$\begin{array}{c} \uparrow \quad J_{AF} \downarrow \quad J_F \quad \downarrow J_{AF} \uparrow \quad J_F \uparrow \\ -Cu_1-\ Cu_2-\ Cu_1-\ Cu_2-\ Cu_1- \end{array}$$

copper(II). A gradual increase in $\chi_m T$ is observed as the temperature is decreased ($\chi_m T$ = 0.888 cm^3 K mol^{-1} at 38.06 K), indicating the presence of a net weak ferromagnetic intrachain interaction.

Magnetostructural data of the complex allow us to foresee two kinds of magnetic exchange couplings within the 1D network (Scheme 1). Consequently, the magnetic data for **1** was analyzed with the Hamiltonian $\hat{H} = -J\sum(\hat{S}_{2i}\hat{S}_{2i-1} - \alpha\hat{S}_{2i}\hat{S}_{2i+1})$, where J is the coupling parameter associated with a particular copper(II) pair and αJ is the exchange consistent associated with the adjacent unit (the alternating parameter α being defined as $J_F/|J_{AF}|$). To analyze the magnetic data, we used a numerical expression for an alternating ferro- and antiferromagnetic Heisenberg chain derived by Georges et al.[42] The numerical expression used to fit the experimental data is given in the following equations:

$$\chi_M = (Ng^2\beta^2/2kT)\, F(\alpha,x) \tag{1}$$

$$F(\alpha,x) = (A_1x^4 + A_2x^3 + A_3x^2 + A_4x)/(x^4 + A_5x^3 + A_6x^2 + A_7x + A_8) \tag{2}$$

$$\alpha = J_F/|J_{AF}| \tag{3}$$

$$x = kT/|J_{AF}| \tag{4}$$

$$A_n = \sum_{i=0}^{i=3}\alpha_{ni}\alpha^i \tag{5}$$

where α^i denotes the ith power of α, i.e., $\alpha^i = (J_F/|J_{AF}|)^i$. The corresponding α_{ni} values, valid in the range $0 \leq \alpha \leq 5$, are listed in Table 7.

The least-squares fit from eq 1 to the data was found with J_{AF} = −191.0 cm^{-1}, J_F = 291.1 cm^{-1}, and g = 2.19. The agreement factor, defined as $F = \Sigma_i(\chi_i^{obs} - \chi_i^{calcd})^2/(\chi_i^{obs})^2$, was 1.096 × 10^{-4}, for all of the 96 observations. This result indicates that a net ferromagnetic intrachain interaction exists in the alternating N₃$^-$ bridged chain.

(40) Goher, M. A. S. *Rev. Inorg. Chem.* **1985**, *7* (4), 299.
(41) Cortes, R.; Drillon, M.; Solans, X.; Lezama, L.; Rojo, T. *Inorg. Chem.* **1997**, *36*, 677.
(42) Borras-Almenar, J. J.; Coronado, E.; Currrely, J.; Georges, R.; Gianduzzo, J. C. *Inorg. Chem.* **1994**, *33*, 5171.
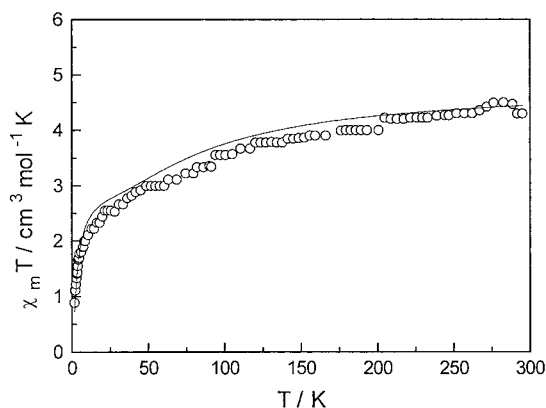
Figure 4. Plots of the products $\chi_m T$ vs temperature for [CuMn(4,4'-dmbpy)$_2$(N$_3$)$_4$]$_n$. The solid line represents the best fitting (see text for the fitted parameters).

Table 7. The Corresponding α_{ni} Values ($0 \le \alpha \le 5$)

|	$i = 0$	$i = 1$	$i = 2$	$i = 3$
$n = 1$	1	0	0	0
$n = 2$	5	0	0	0
$n = 3$	−1	0	0	0
$n = 4$	0.5	0	0	0
$n = 5$	5.32559	−1.15923	0.34561	−0.03731
$n = 6$	0.49591	−0.01920	−0.01617	−0.00795
$n = 7$	0.03123	0.48241	−0.16542	0.01445
$n = 8$	0.33563	−0.34155	0.09592	−0.08846

**Scheme 2.** The Relationship of the Magnetic Exchange Coupling of **6**.
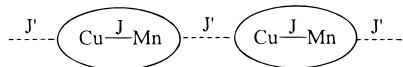
The magnetic behavior of [CuMn(4,4'-dmbpy)$_2$(N$_3$)$_4$]$_n$ (**6**) is represented in Figure 4. The observed $\chi_m T$ value is 4.47 cm^3 K mol^{-1} at 292.5 K, which is slightly lower than the spin-only value of 4.75 cm^3 K mol^{-1} for an uncoupled Cu(II) and Mn(II) unit. A gradual decrease in $\chi_m T$ is observed while the temperature is decreased, indicating the presence of an antiferromagnetic interaction in this compound.

To interpret the magnetic behavior of **6**, we used an approximation for the system shown in Scheme 2.[43] As indicated in Scheme 2, complex **6** can be considered as a uniform chain formed by Mn−(N$_3$)$_2$−Cu binuclear units:

$$\cdots\cdots S_{eff} \overset{J'}{\cdots\cdots} S_{eff} \overset{J'}{\cdots\cdots} S_{eff} \cdots\cdots$$
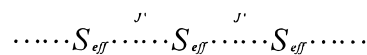
where S_{eff} symbolizes the effective spin of heterobinuclear unit

$$(\text{Cu}^{\text{II}} \overset{J'}{\text{——}} \text{Mn}^{\text{II}})$$
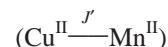
On the assumption of purely isotropic interactions, the susceptibility of the binuclear unit (Cu$^{\text{II}}$−Mn$^{\text{II}}$) χ_b is calculated from eq 6.

$$\chi_b = \chi_{\text{Cu−Mn}} = (Ng^2\beta^2/kT)\{[10\exp(-6J/kT) + 28]/[5\exp(-6J/kT) + 7]\} \quad (6)$$

Assuming that S_{eff} is treated as a classical spin and $g_{eff} = 2$, S_{eff} can be calculated from eq 7, and the magnetic susceptibility of chain can be described by the classical spin model (eq 8) derived by Fisher.[44]

$$S_{eff}(S_{eff} + 1) = 3k(\chi_b T)/Ng_{eff}^2\beta^2 \quad (7)$$

$$\chi_M = [Ng^2\beta^2 S_{eff}(S_{eff} + 1)/3kT](1 + u)/(1 - u) \quad (8)$$

with $u = \coth[J'S_{eff}(S_{eff} + 1)/kT] - kT/J'S_{eff}(S_{eff} + 1)$

The least-squares fit from eq 8 to the data was found with $J = J_{AF} = -15.45$ cm^{-1}, $J' = J_F = 4.62$ cm^{-1}, $g = 1.99$. The agreement factor, defined as $F = \sum_i(\chi_i^{obs} - \chi_i^{calcd})^2/(\chi_i^{obs})^2$, was 1.528×10^{-3}, for all of the 86 observations. This result indicates that a net antiferromagnetic intrachain interaction exists in **6**.

Supporting Information Available: Tables listing detailed crystallographic data, atomic positional parameters, bond lengths and angles, and figures and crystal data for powder diffraction. This material is available free of charge via the Internet at http://pubs.acs.org.

IC990338Y

(43) Handa, M.; Sayama, Y.; Mikuriya, M.; Nukada, R.; Hiromisu, I.; Kasuga, K. *Bull. Chem. Soc. Jpn.* **1998**, *71*, 119.
(44) Fisher, M. E. *Am. J. Phys.* **1964**, *32*, 343.